J Soils Sediments (2013) 13:344–353
DOI 10.1007/s11368-012-0612-z

SOILS, SEC 3 • REMEDIATION AND MANAGEMENT OF CONTAMINATED OR DEGRADED LANDS • RESEARCH ARTICLE

Sorption isotherms and kinetics of Sb(V) on several Chinese soils with different physicochemical properties

Jian-Xin Fan · Yu-Jun Wang · Xiao-Dan Cui · Dong-Mei Zhou

Received: 18 June 2012 / Accepted: 24 September 2012 / Published online: 6 October 2012

Abstract

Purpose Sorption of antimony on soils is the primary factor that influences its immobilization and migration in the environment. In the present study, the sorption of Sb(V) onto seven Chinese soils with different physicochemical properties was investigated for exploring the relationship between the sorption capacity of Sb(V) and the physicochemical properties of the soils.

Materials and methods Sorption isotherms and kinetics experiments were performed to ascertain the sorption capacity and the kinetic rate, respectively. The relationship between the sorption capacity of Sb(V) and the physicochemical properties of the soils was analyzed by multiple linear regressions.

Results and discussion The results showed that the sorption isotherms fitted with both the Langmuir and Freundlich equations very well (R^2=0.936–0.997), and the sorption kinetic of Sb(V) onto the seven Chinese soils followed a pseudo-second-order reaction. The maximum sorption capacity of Sb(V) on the soils ranged from 134 to 1,333 $\mathrm{mg\,kg^{-1}}$. Nearly 94 % of the variability in maximum sorption of Sb(V) modeled by Freundlich equation could be described by $\mathrm{Fe_{DCB}}$ (dithionite–citrate–bicarbonicum extractable), and nearly 98 % of the variability could be described by $\mathrm{Fe_{DCB}}$ and $\mathrm{Al_{DCB}}$.

Conclusions Multiple linear regressions can be successfully applied to analyzing the relationship between sorption capacity and soil properties. $\mathrm{Fe_{DCB}}$ and $\mathrm{Al_{DCB}}$ played important roles in Sb(V) sorption onto soils. It would be useful to understand the environmental behaviors of Sb and for the implementation of risk assessment management and remediation strategies of Sb.

Keywords $\mathrm{Al_{DCB}}$ · Antimony sorption · $\mathrm{Fe_{DCB}}$ · Langmuir isotherm · Soil properties

1 Introduction

Antimony is the ninth most mined metal for industrial uses in the world. It is used in large quantities (>100,000 tons annually worldwide) in a variety of industrial products, especially flame retardants and catalysts in the synthesis of plastics, and alloys for ammunition ((Ettler et al. 2007); (Filella et al. 2002a); (Hammel et al. 2000); (Krachler & Emons 2001); (Mitsunobu et al. 2010)). Moreover, China is rich in Sb mineral resources, and the largest Sb deposit in the world is located in Lengshuijiang City, Hunan Province, China, named Xikuangshan Sb mine ((He 2007); (Qi et al. 2011)). Chinese scientists had discussed the antimony pollution in China so far ((Diao et al. 2010); (He & Wan 2004); (Qi et al. 2008); (Qi et al. 2011)) and found that there were 114 Sb mines located within 18 provinces or autonomous regions. The present annual demand for Sb on the international market was predicted as approximately 90,000 tons, and the annual domestic demand in China was roughly 10,000 tons, totaling about 100,000 tons per annum (He et al. 2012). Therefore, China plays an important role in global anthropogenic emission of Sb, and severe environmental contamination of Sb has been reported in some areas ((Diao et al. 2010); (Qi et al. 2008); (Qi et al. 2011)).

Antimony is a toxic element, and widely exists in water, soil, and air (Filella et al. 2002a). The pollution sources of antimony are classified as artificial source and natural source,

Responsible editor: Jean-Paul Schwitzguébel

J.-X. Fan · Y.-J. Wang · X.-D. Cui · D.-M. Zhou (✉)
Key Laboratory of Soil Environment and Pollution Remediation,
Institute of Soil Science, Chinese Academy of Sciences,
Nanjing 210008, People's Republic of China
e-mail: dmzhou@issas.ac.cn

J.-X. Fan · X.-D. Cui
Graduate School of Chinese Academy of Sciences,
Beijing 100049, People's Republic of China

and the primary sources come from anthropogenic activities and the extensive use of Sb compounds ((Filella et al. 2007); (Smichowski 2008)). Antimony exists in a variety of oxidation states (−III, 0, III, V), and the oxidation states are the most common inorganic species in the natural environment, while $Sb(OH)_3$ and $Sb(OH)_6-$ are the dominant chemical species in wet environments. In general, inorganic Sb compounds are found to be more toxic than organic Sb, and Sb(III) is more toxic than Sb(V) ((Filella et al. 2002b); (Okkenhaug et al. 2011)). According to thermodynamic equilibrium predictions, antimony exists as Sb(V) in oxic systems and as Sb(III) in anoxic systems (Filella et al. 2002a). However, even under reducing conditions, X-ray absorption studies on mine soil samples have shown that antimony was adsorbed as Sb(V) instead of Sb(III) ((Mitsunobu et al. 2005); (Mitsunobu & Takahashi 2008)).

Even though antimony is identified as a toxic chemical entering into the environment, there are only limited literatures focusing on its environmental behaviors. Sorption plays a vital role in antimony immobilization and migration in soils. The specific sorption of Sb(V) by synthesized Mn oxyhydroxides, Al hydroxides, and Fe oxyhydroxides was investigated in many precious studies ((Ilgen & Trainor 2012); (Leuz et al. 2006b); (Rakshit et al. 2011)). Additionally, many scientists obtained some results that metal oxides and metal hydroxides had a very high affinity for antimony ((Leuz et al. 2006a); (Martínez-Lladó et al. 2011); (Nakagawa et al. 2005); (Tighe et al. 2005a); (Watkins et al. 2006)), and the presence of these minerals seemed to be responsible for high sorption capacity of some soils ((Martínez-Lladó et al. 2011); (Mitsunobu et al. 2010); (Nakamaru et al. 2006); (Takaoka et al. 2005); (Tighe et al. 2005a)).

Few studies have examined the dominant components of natural soil which contributed to the sorption of antimony. (Tighe et al. 2005b) investigated adsorption behavior of Sb (V) by two organic-rich soils, amorphous phases ($Fe(OH)_3$) and humic acid, and found that sorption capacity of Sb(V) on the amorphous iron was much higher than that on humic acid, and soil with high amorphous iron content has higher sorption capacity. (Johnson et al. 2005) studied the antimony sorption on the soils of a shooting range in Switzerland, and found that 40–70 % of antimony was bound to amorphous ferrihydrite of acid-soluble components. Even though antimony sorption on soils was influenced by amorphous ferrihydrite content in the soil, the dominant component of natural soil which contributes to the sorption of antimony is not very clear.

In this study, the sorption of antimony on seven Chinese soils with different physicochemical properties was investigated to explore the relationship between the sorption capacity of Sb and the physicochemical properties of the soils by multiple linear regressions. Such information would be useful to understand the environmental behaviors of Sb and for the implementation of risk assessment management and remediation strategies of Sb.

2 Materials and methods

2.1 Soils

Seven surface soil samples (0–20 cm) with different geological environments were collected from the cultivated land away from industrial sites. Soil samples were air-dried, homogenized, and ground to pass 0.25-mm nylon fiber sieve for the further sorption experiments.

Soil pH values were determined with a commercial glass electrode (REX, pHS-3B) after equilibration of 8 g of soil with 20 ml of deionized water (CO_2 was removed). The cation exchange capacities of the soils (CEC) were determined as the sum of the basic cations and Al extracted with 0.1 M $BaCl_2$ and the extractable acidity (Sumner & Miller 1996). Organic matter (OM) content was determined by titration with $FeSO_4$ after oxidized by $K_2Cr_2O_7$ and concentrated H_2SO_4 in the condition of external heat (Allison 1960). Soil texture was determined by a LS 230 laser diffraction particle analyzer (Beckman Coulter). Total soil Fe, Al, and Mn were analyzed by digesting the soils with a mixture of HF, $HClO_4$, and HNO_3 with a ratio of 3:1:1 at 240 °C. The quality assurance of the analytical procedure was checked by routinely analyzing certified reference materials and including blanks in digestion batches (Luo et al. 2006). Total antimony in soil was determined by hydride generation atomic fluorescence spectrometry (Beijing Haiguang, China) after digestion of soils with 3:1 (*v*/*v*) HNO_3/HCl (nitrohydrochloric acid) at boiling water bath. Amorphous (weak crystalline) soil Fe, Al, and Mn were extracted by shaking 1 g of soil in 30 ml of acidified ammonium oxalate buffer (0.175 $mol L^{-1}$ $(NH_4)_2C_2H_4$+ 0.1 $mol L^{-1}$ $H_2C_2O_4$, pH 3.0) for 2 h (Loeppert et al. 1996). Free soil Fe, Al, and Mn oxides were extracted by dithionite–citrate–bicarbonicum (DCB) standard procedure (Mehra & Jackson 1960). Concentrations of Fe, Al, and Mn were determined by inductively coupled plasma atomic emission spectrometry (RIS Advantage). All measurements were repeated in triplicate.

2.2 Sorption experiments

Antinomy(V) stock solutions were prepared from $K_2H_2Sb_2O_7 \cdot 4H_2O$. All working standards and initial solution for antinomy sorption isotherms and kinetic experiments were prepared by a serial dilution with deionized water. A batch equilibration method was conducted for the study of sorption isotherms of antinomy in all sorption experiments. Ionic strength was kept constant at 10 mmolL^{-1} in all the experiments by means of NaCl addition, and pH was adjusted to 5.5 by MES (2-(*N*-morpholino) ethanesulfonic acid hydrate) buffer. Samples of 1 g of soil were put in contact with 25 mL of an aqueous solution of antimony (initial concentrations ranging from 0 to 29.3 mgL^{-1}) in polyethylene tubes. After shaking reciprocation for 24 h (25±1 °C) and centrifuging at 9,000 rpm, supernatant liquid was filtered by using 0.45-μm cellulose filters before analysis. Concentration of Sb in the supernatant was determined by atomic fluorescence spectrometer (Beijing Haiguang). All the sorption experiments were performed in duplicate.

Sorption kinetic experiments were performed in order to obtain sorption as a function of time. Dynamic contacts were carried out in polyethylene tubes. To a given reaction time, each sample was collected from one of the tubes, which will not be used again. In the experiments, the initial antimony concentration was 0.61 mgL^{-1}, and samples were performed from 0 to 48 h.

The amount of sorption at equilibrium, Q (milligrams per kilogram), was calculated as

$$Q = (C_0 - C_e) \times V/W \tag{1}$$

Where C_0 and C_e are the initial liquid-phase concentrations of Sb(V) and at equilibrium (milligrams per liter), respectively; Q is the equilibrium sorption capacity (milligrams per kilogram); V is the volume of the solution (liters); and W is the mass of the adsorbent (grams). All the sorption experiments were performed in duplicate.

2.3 Sorption models

2.3.1 Sorption isotherm

Langmuir and Freundlich equations were used to describe the sorption isotherms of Sb(V) on soils. The Langmuir equation is a valid monolayer sorption on a surface containing a finite number of binding sites. It assumes uniform energies of sorption on the surface and no transmigration adsorbate in the plane of the surface. The Langmuir equation is written as

$$Q = KQ_M C/(1 + KC) \tag{2}$$

where C is the equilibrium concentration of antimony in the bulk solution (milligrams per liter), Q is the equilibrium content in solid phase (milligrams per kilogram), Q_M (milligrams per kilogram) and K (liters per milligram) are maximum sorption capacity and sorption energy, respectively. The maximum sorption capacity (Q_M) represents the complete monolayer coverage of adsorbent with antimony, and K represents the enthalpy of sorption and varies with temperature.

The Freundlich equation is an empirical sorption model that can be expressed as

$$Q = KC^N \tag{3}$$

Where Q and C are defined previously, K is a Freundlich's constant related to the sorption capacity, and N is considered to be the relative indicator of sorption intensity.

2.3.2 Sorption kinetics

In this paper, sorption kinetic data were simulated by the pseudo-first-order rate equation, pseudo-second-order rate equation, Elovich equation, and double-constant rate equation. The kinetic equations can be expressed as follows:

Pseudo-first-order rate equation:

$$\frac{dQ_t}{dt} = K_1(Q_e - Q_t) \tag{4}$$

Eq. (4) can be expressed as:

$$Q_t = Q_e\left(1 - e^{-k_1 t}\right) \tag{5}$$

Pseudo-second-order rate equation:

$$\frac{t}{Q_t} = \frac{1}{{Q_e}^2 K_2} + \frac{1}{Q_e K_2} t \tag{6}$$

Elovich equation:

$$Q_t = \frac{1}{K} \ln(1 + \alpha K t) \tag{7}$$

Double constant equation:

$$Q_t = at^b \tag{8}$$

Where Q_t is the amount of Sb(V) adsorbed (milligrams per kilogram) at time t (hours), Q_e is the amount adsorbed (milligrams per kilogram) at equilibrium time and a, b, K_1, K_2, α, and K are the sorption constant. In this paper, fitting of sorption isotherms and sorption kinetics data, and the calculation of the parameters in all equations were undertaken by nonlinear regression using SigmaPlot 12.0.

3 Results and discussion

3.1 Physicochemical properties of the soils

The soils used in this paper were collected from different sites throughout China, and were classified as Alfisols, Ultisols, Inceptisols, and Mollisols according to American soil taxonomy (Jiang et al. 2005a). The details were shown in Table 1. As shown in Table 1, there are wide differences in the physicochemical properties of the seven soils. First of

Table 1 Location, classification, and some properties of soils

Soil classification	Jiangsu (Alfisols)	Henan (Alfisols)	Shandong (Alfisols)	Guangdong (Ultisols)	Hunan (Ultisols)	Sichuan (Inceptisols)	Heilongjiang (Mollisols)
pH (1:2.5)	5.5	8.5	7.8	4.9	5.0	8.1	6.0
CEC (mmol kg^{-1})	156	92.0	209	95	134	217	348
DOC (mg kg^{-1})	95.2	64.3	92.6	7.72	38.8	73.5	185
OM (%)	1.45	0.62	1.46	0.0878	1.51	0.956	4.34
Fe_{total} (%)	7.10	6.76	10.2	10.8	11.4	7.56	8.57
Al_{total} (%)	13.5	18.1	18.5	2.52	30.4	11.7	23.79
Mn_{total} (%)	0.158	0.131	0.194	0.0321	0.122	0.116	0.253
Fe_{OX} (%)	0.597	0.180	0.193	0.154	0.368	0.188	0.771
Al_{OX} (%)	0.211	0.0846	0.204	0.234	0.406	0.125	0.369
Mn_{OX} (%)	0.0700	0.0220	0.0575	0.0655	0.0242	0.0452	0.0988
Fe_{DCB} (%)	2.80	2.08	2.71	6.05	5.69	3.37	2.43
Al_{DCB} (%)	0.275	0.102	0.234	0.904	1.02	0.198	0.395
Mn_{DCB} (%)	0.129	0.0968	0.0665	0.0323	0.0807	0.0439	0.0542
Sb (mg/kg)	1.09	1.02	1.03	3.41	2.87	1.15	0.61
Clay (%)	14.8	7.12	14.7	21.9	15.1	20.1	16.05
Silt (%)	71.6	42.9	73.9	45.0	77.1	66.6	71.00
Sand (%)	13.6	49.9	11.4	33.1	7.8	13.3	12.91

Fe_{OX} amorphous Fe, Al_{OX} amorphous Al, Mn_{OX} amorphous Mn extracted by acidified ammonium oxalate buffer; Fe_{DCB} DCB-extractable Fe, Al_{DCB} DCB-extractable Al, Mn_{DCB} DCB-extractable Mn

all, the pH of these soils ranged from 4.9 to 8.5, and soil organic matter contents varied significantly. The lowest content was 0.0878 % in Guangdong soil, and the highest one was 4.34 % in Heilongjiang soil. Additionally, the total Fe, Al, and Mn varied considerably in the tested soils. DCB-extractable Fe content of these soils ranged from 2.08 to 6.05 %, and Ultisols had high content of Fe_{DCB}. Moreover, the soil textures were also different, and all the different physicochemical properties could affect the sorption of antimony on the soils.

3.2 Sorption kinetic of Sb(V) on the soils

Sorption kinetic is important to be able to predict the rate at which contamination is fixed onto soils. The results of the variation of the Sb(V) sorption onto the seven different soils with time were shown in Fig. 1. In some soils (Guangdong and Hunan soils), the sorption seems to be relatively quick, but in the other ones (such as Jiangsu and Shandong soils), the equilibrium was reached even after several hours. This difference could be due to the different iron content in the soils studied. For example, Guangdong and Hunan soils that reached the equilibrium only few minutes after the contact with Sb(V) had the highest total and DCB-extractable iron content (see Table 1). Thus, the equilibrium time could be influenced by DCB-extractable iron content. Meanwhile, (Martínez-Lladó et al. 2011) investigated Sb(V) adsorption and migration in several calcareous soils, and obtained that the higher iron content in the soil, the adsorption reaction equilibrium reached faster.

In this work, kinetic data were modeled by four widely used equations (pseudo-first-order rate equation, pseudo-second-order rate equation, Elovich equation, and double-constant rate equation). When the pseudo-first-order rate equation and Elovich equation were employed to fitting the experimental data, as shown in Table 2, the correlation coefficients changed in the range of 0.629–0.997 and 0.447–0.967, respectively. The results indicated that the experimental data did not agree with the pseudo-first-order kinetic model and Elovich equation.

Pseudo-second-order equation has been widely used to describe trace element sorption in different adsorbents (Shen et al. 2009). The values of the kinetic constants of two kinetic models were shown in Table 2. Pseudo-second-order rate equation provided a good fitting and described properly the sorption process, and the correlation coefficients were 0.994 to 0.999. Figure 2 showed both the experimental data and the pseudo-second-order model obtained by Eq. (6), and the plots of t/Q_t against t gave straight lines. Additionally, as shown in Table 2, double-constant rate equation also provided a well fitting to the experimental data. The correlation coefficients reported were above 0.960.

In general, fitting of model to the data points indicated that the sorption of Sb(V) onto the seven different soils followed a pseudo-second-order reaction. (Martínez-Lladó

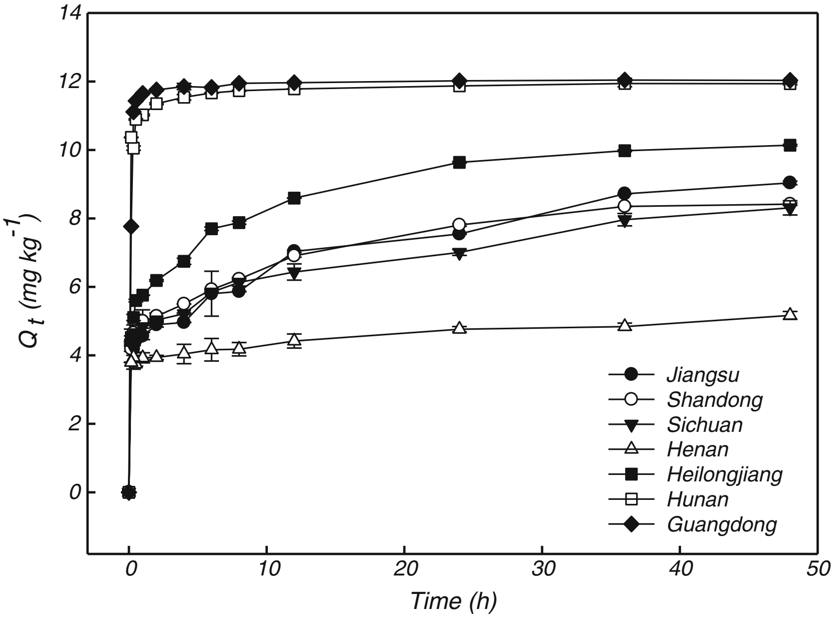

Fig. 1 Sorption of antinomy (V) on the seven different soils as a function of contact time, with reaction conditions: ionic strength (I)=0.01 molL^{-1} NaCl, pH=5.5, T=298 K, initial antinomy(V) concentration (C_0)=0.61 mgL^{-1}, and m/v of soil to solution=1 g/25 ml

et al. 2011) also found that the sorption kinetic of Sb on the soils followed the pseudo-second-order model very well. Additionally, the sorption rate of Guangdong soils was the fastest among all the soils due to its highest content of Fe$_{\mathrm{DCB}}$, This phenomena demonstrated that the fast sorption of Sb(V) on the soils was due to high content of iron oxy-hydroxides.

3.3 Batch sorption of Sb(V) on soils

The variation of Sb(V) sorption as a function of Sb(V) concentration in the solution at equilibrium was shown in Fig. 3. Sorption of Sb(V) on all the soils increased with the increasing solution Sb(V). Wide differences in Sb(V) sorption were obtained among the seven soils. The sorption capacities of Sb on the Guangdong and Hunan soils were much higher than those on the other soils, and the sorption capacity of Sb on the Henan soil was the lowest.

Langmuir and Freundlich models were used to fit the experimental data, and the nonlinear forms of Langmuir equation for the sorption data were shown in Fig. 3. Some parameters on sorption energy and capacity were estimated by the fitted nonlinear equations of Langmuir and Freundlich models, as shown in Table 3. High regression coefficients (>0.936) for all cases revealed that two models were well fitted to the sorption of Sb(V) on the seven soils. In addition, the regression coefficients for Langmuir model ($0.991<R^2<0.998$) were higher than those for Freundlich ($0.936<R^2<0.990$), indicating a better fitting with the Langmuir. For the Langmuir equation, predicted sorption capacities (Q_{MAX}) ranged from a low of 143 mgkg^{-1} on the Henan soil to a high of 1,333 mgkg^{-1} on the Guangdong soil.

The sorption capacities of seven experimental soils were very different, which is due to their different physiochemical properties. In general, the sorption capacities could be related to the higher content of sesquioxides (Fe and Al) and high OM. From Table 1, the total Fe contents in the Guangdong and Hunan soils were very high, which may result in the higher maximum sorption of Sb(V) on these

Table 2 Regressed kinetic parameters for antimony adsorption on the seven soils

	Double constant			Pseudo-first-order model			Pseudo-second-order model			Elovich		
Soil	a	b	R^2	Q_e	K_1	R^2	Q_e	K_2	R^2	α	K	R^2
Jiangsu	4.62	0.161	0.980	6.54	3.09	0.629	1.82	0.0611	0.994	236	1.16	0.854
Shandong	4.96	0.134	0.992	6.59	3.68	0.725	1.28	0.0920	0.995	628	1.32	0.916
Guangdong	10.9	0.0366	0.968	11.9	6.733	0.997	0.0542	1.53	0.999	3.51×10^8	1.89	0.447
Hunan	10.9	0.0277	0.999	11.4	6.73	0.976	0.0920	0.910	0.999	4.68×10^8	1.93	0.524
Sichuan	4.81	0.128	0.989	6.29	3.93	0.718	1.40	0.0872	0.996	863	1.44	0.898
Henan	3.94	0.0539	0.990	4.30	11.6	0.893	0.713	0.277	0.997	1.67×10^7	4.58	0.809
Heilongjiang	5.85	0.147	0.997	8.19	2.67	0.763	1.12	0.0874	0.997	349	0.972	0.967

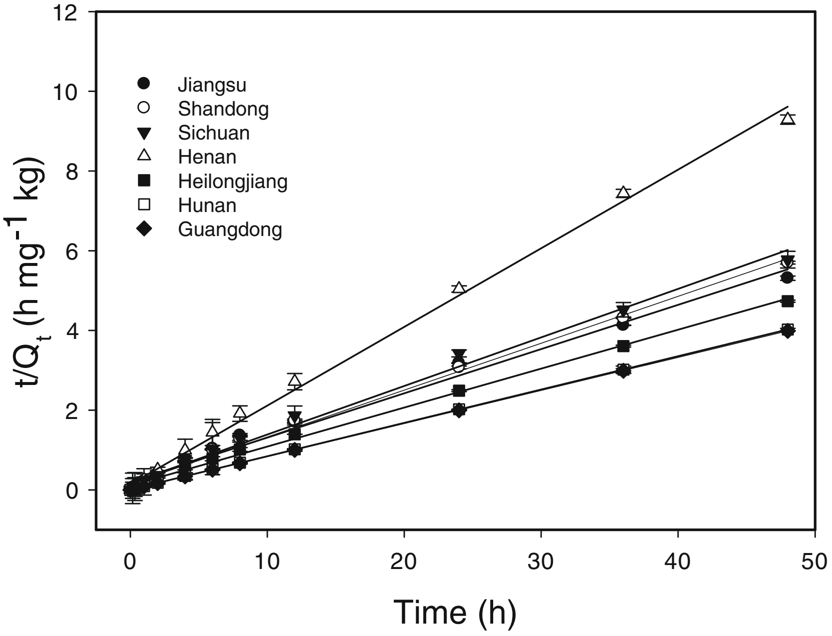

Fig. 2 Pseudo-second-order kinetics for antinomy(V) sorption on the seven different soils; *markers* are experimental data and *lines* are the data predicted by pseudo-second-order kinetics model

two soils. In addition, soil organic matters including humic acid and fulvic acid influenced the adsorptive reaction. Sb (V) could be bound onto OM by complexing action (as Sb-OM), at the same time, OM also affects Sb(V) sorption onto clay by forming the Sb-OM-clay (Xi et al. 2010). For example, a high value of maximum sorption of Sb(V) found in Heilongjiang soil (974 mg/kg) could be also correlated with the highest OM content (4.34 %) when compared with the same parameters with other soils. Moreover, the texture of soils can also affect Sb(V) sorption onto soils. In conclusion, Sb(V) sorption would have related with the physicochemical properties of the soils, especially like OM, clay, and Fe (Al) oxides. Similar phenomena were observed for phosphate and arsenic sorption ((Börling et al. 2001); (Jiang et al. 2005a); (Jiang et al. 2005b); (Kang et al. 2009); (Ruiz et al. 1997))

3.4 Impacts of soil properties

A model was made to explain the relationship between sorption capability and soil properties, in order to identify the most important factor affecting Sb(V) sorption on soils. In general, maximum sorption was used to express the soil ability to immobilize Sb(V), or redistribute, and the likely potential for release of adsorbed Sb(V) into soil solution. Hence, the relationship between maximum sorption modeled by Langmuir

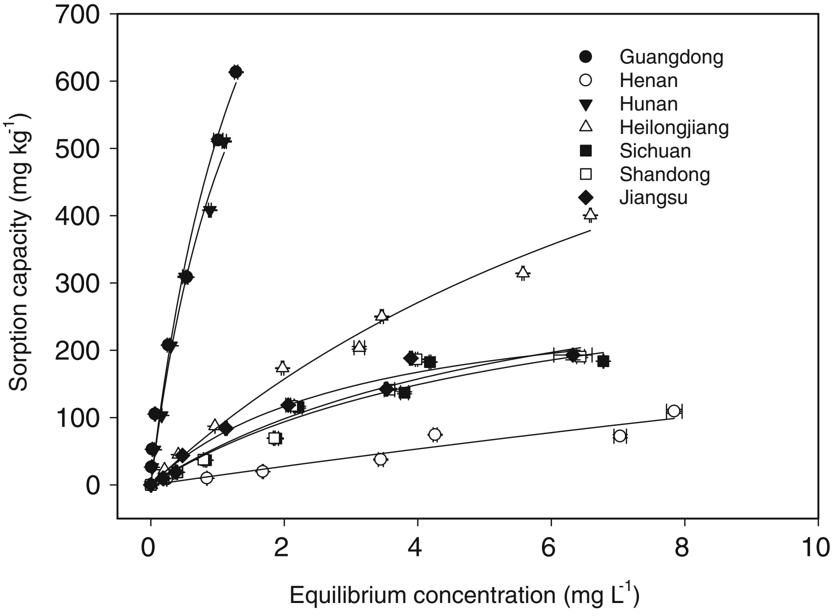

Fig. 3 Sorption isotherms of antinomy (V) on the seven different soils. *Markers* are experimental data, and *lines* are the data predicted by Langmuir model. Reaction conditions: ionic strength (I)=0.01 molL^{-1} NaCl, pH=5.5, T=298 K, and m/v of soil to solution=1 g/25 ml

Table 3 Langmuir and Freundlich equation parameters calculated using nonlinear curve fitting for adsorption isotherms of seven soils

Soil	Langmuir			Freundlich		
	K ($\mathrm{Lmg^{-1}}$)	Q_{MAX} ($\mathrm{mgkg^{-1}}$)	R^2	$1/n$	K_{f} ($(\mathrm{mgkg^{-1}})(\mathrm{mgL^{-1}}))^{-1/n}$	R^2
Jiangsu	0.327	295	0.997	0.595	70.9	0.954
Shandong	0.165	396	0.998	0.701	57.6	0.940
Guangdong	0.636	1333	0.992	0.672	509	0.995
Hunan	0.703	1133	0.994	0.735	469	0.994
Sichuan	0.173	365	0.991	0.683	55.5	0.937
Henan	0.143	143	0.994	0.610	20.9	0.936
Heilongjiang	0.096	974	0.996	0.751	93.1	0.990

and Freundlich equations and the most important soil characteristics was investigated by stepwise regression analysis. The total independent variables examined in the regression procedure were pH, DOC, OM, total Fe, Al, Mn and P, oxalate-extractable soil Fe, Al, and Mn, dithionite–citrate–bicarbonicum-extractable soil Fe, Al, and Mn, and soil texture. The regression results including the coefficient correlations and p values were reported in Table 4. In general, the p values can be regarded as the probability of getting a correlation as large as the observed value by random chance, when the true correlation is zero. Correlations with p values lower than 0.05 have been considered significant (Martínez-Lladó et al. 2011). As shown in Table 4, there were positive correlations between the total Fe, Al, $\mathrm{Fe_{DCB}}$, and $\mathrm{Al_{DCB}}$ and the Q_{MAX} and K_{f}, and the p values were significantly lower than 0.05. Additionally, their correlation coefficients were greater than 60 %, and interesting results were that dithionite–citrate–bicarbonicum-extractable soil Fe and Al expressed the best correlation with the K_{f}, and correlation coefficients were greater than 90 %. On the other hand, the results in Table 4 also showed the negative correlations between Q_{MAX} and K_{f} and total P, pH, DOC, and $\mathrm{Mn_{OX}}$. However, the p values are not lower than 0.05.

Table 4 Correlation coefficient and p values of Q_{MAX} and K_{f} related to the physicochemical properties of the soils

	Q_{MAX}		K_{f}	
	Correlation coefficient	p	Correlation coefficient	p
$\mathrm{Al_{total}}$	0.673	0.024	0.627	0.034
$\mathrm{Fe_{total}}$	0.627	0.034	0.662	0.026
$\mathrm{Mn_{total}}$	0.071	0.561	0.392	0.133
$\mathrm{Al_{DCB}}$	0.817	0.005	0.956	0.001
$\mathrm{Fe_{DCB}}$	0.644	0.020	0.942	0.001
$\mathrm{Mn_{DCB}}$	0.004	0.963	0.002	0.931
$\mathrm{Al_{OX}}$	0.577	0.047	0.296	0.207
$\mathrm{Fe_{OX}}$	0.027	0.723	0.031	0.706
$\mathrm{Mn_{OX}}$	−0.048	0.635	−0.387	0.135
$\mathrm{P_{Total}}$	−0.448	0.100	−0.675	0.023
Clay	0.373	0.145	0.230	0.275
pH	−0.631	0.033	−0.559	0.053
DOC	−0.040	0.663	−0.401	0.127
OM	0.028	0.719	0.079	0.541

As shown in Table 4, $\mathrm{Fe_{DCB}}$ and $\mathrm{Al_{DCB}}$ played important roles in the Sb(V) sorption onto the seven soils by studying their relationship with maximum sorption amount modeled by Langmuir equation, and nearly 64 and 82 % of the variability in the maximum sorption of Sb(V) could be described. It is described that $\mathrm{Fe_{DCB}}$ and $\mathrm{Al_{DCB}}$ were the controlling factors for Sb(V) sorption in the seven soils. At the same time, good relationship between K_{f} simulated by Freundlich equation and the physicochemical properties of soils was obtained. As Table 4 and Fig. 4 described, the better dependence between K_{f} and $\mathrm{Fe_{DCB}}$ ($\mathrm{Al_{DCB}}$) was obtained. Nearly 95 % of the variability in maximum sorption of Sb(V) on the soil surface could be described by $\mathrm{Fe_{DCB}}$ or $\mathrm{Al_{DCB}}$. Dithionite–citrate–bicarbonicum agent was able to dissolve a large proportion of crystalline iron oxides as well as amorphous iron oxides, while oxalate extraction was able to dissolve most of the amorphous iron oxides. Therefore, the crystalline iron oxides played more important role in the Sb(V) sorption.

As we know, the sorption capacity can be impacted by many factors. Hence, the relationship between sorption maximum and soil properties was studied by multiple linear regressions, as shown in Table 5. The best equations were listed as follows:

$$K_f = 326.4[Al_{DCB}] + 59.2[Fe_{DCB}] - 178 \quad (R^2 = 0.982,\ p < 0.001) \tag{9}$$

The regression results showed that soil organic matter also had a positive effect on Sb(V) sorption. Soil organic matter could react with Sb(V) under an environmentally relevant condition. Over 30 % of total Sb(III) could be bound to natural organic matter in the soils (Buschmann & Sigg 2004), and the same phenomenon could be produced when Sb(V) was added

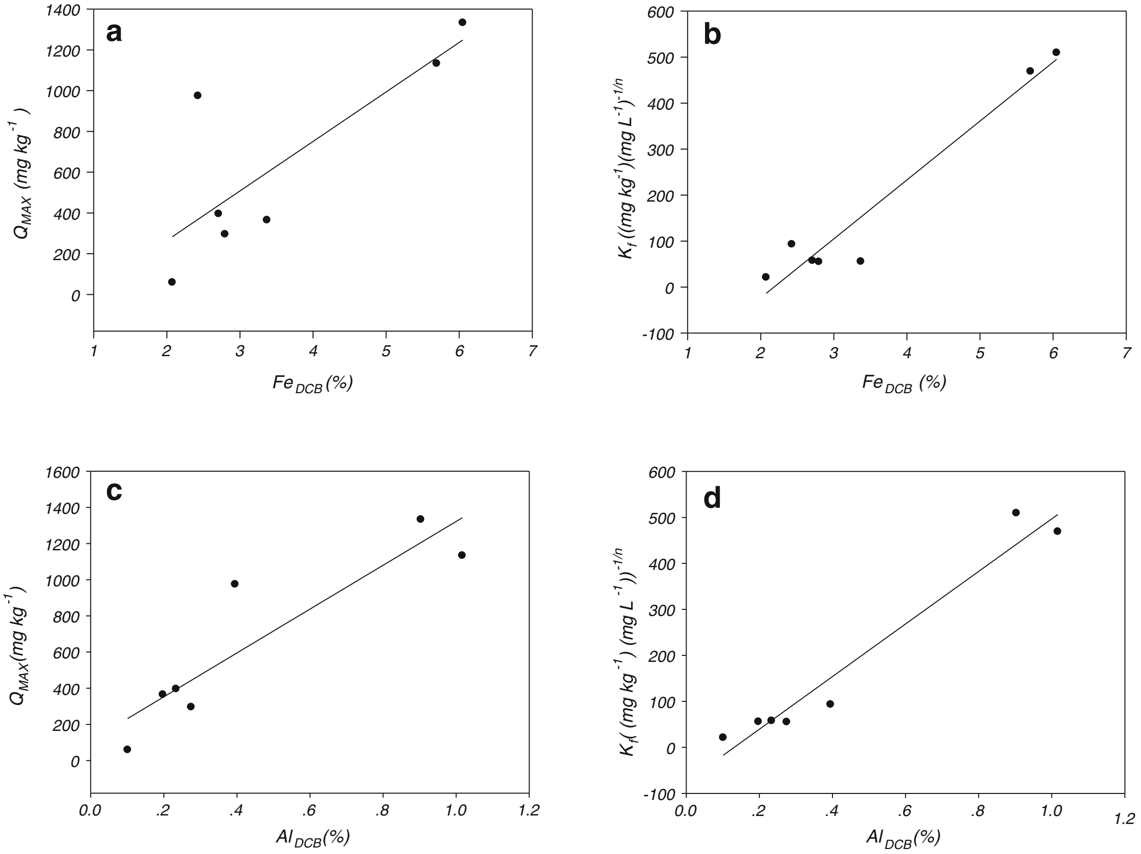

Fig. 4 Relationship between maximum sorption capacity and Fe_{DCB} (Al_{DCB}). **a** The relationship between the Q_{MAX} and Fe_{DCB}. **b** The relationship between K_f and Fe_{DCB}. **c** The relationship between the Q_{MAX} and Al_{DCB}. **d** The relationship between K_f and Al_{DCB}

to soils. Therefore, soil organic matter affected the immobility of Sb(V) in soils.

The effect of soil texture was also considered, and clay content promoted the sorption capacity. It was ascribed to more sorption sites included in the soil with more high content of clay. On the other hand, soils containing higher percentage of clay would have high surface areas, which is important for sorption. There were negative correlations between Q_{MAX} and K_f, total P and pH because the P fixed in soil can occupy the sorption sites. The pH affected the sorption capacity because the soil with lower pH has more positive charges which can attract chemical with more negative charges, such as $Sb(OH)_6^-$. However, the result showed that clay content was less important than Fe_{DCB} and Al_{DCB} for Sb(V) sorption. Additionally, other soil properties did not exhibit significant impacts.

Table 5 Model summary

Model	Multiple linear equation	R^2
The stepwise regression for Q_{MAX}		
1	Q_{MAX}=243[Fe_{DCB}]-221	0.644
2	Q_{MAX}=1,213[Al_{DCB}]+110	0.817
3	Q_{MAX}=1,634[Al_{DCB}]+101.8 [Fe_{DCB}]+287	0.832
The stepwise regression for K_f		
1	K_f=128 [Fe_{DCB}]−279	0.942
2	K_f=57.2[Al_{DCB}]−74.9	0.956
3	K_f=483 [Al_{DCB}]+59.3 [Fe_{DCB}]−178	0.982

4 Conclusions

The different sorption capacity of Sb(V) occurred onto seven Chinese soils. The soil of Guangdong had the highest sorption affinity for the Sb(V), while the soil of Henan had the lowest one. The equilibrium sorption data were fitted by Langmuir and Freundlich isotherm models. The sorption kinetic of Sb onto the soils could be well described by the pseudo-second-order rate equation. Maximum sorption capacity and equilibrium time were influenced by the physicochemical properties of the soils, especially soil Fe_{DCB} and Al_{DCB}. As the multiple linear regression predicted data reported, Fe_{DCB} and Al_{DCB} played important roles in Sb(V) sorption in the soil, and nearly 94 % of the variability in maximum sorption of Sb(V) simulated by Freundlich equation could be described by Fe_{DCB}

(Al_{DCB}). Additionally, nearly 98 % of the variability in maximum sorption of Sb(V) simulated by Freundlich equation on the soil surface could be described by Fe_{DCB} and Al_{DCB}. Other soil properties appeared less important for Sb (V) sorption on soils.

Acknowledgments This work was financially supported by the National Natural Science Foundation of China (nos. 41171189 and 41125007).

References

Allison LE (1960) Wet combustion apparatus and procedure for organic and inorganic carbon in soil. Soil Sci Soc Am Proc 24:36–40

Börling K, Otabbong E, Barberis E (2001) Phosphorus sorption in relation to soil properties in some cultivated Swedish soils. Nutr Cycl Agroecosys 59:39–46

Buschmann J, Sigg L (2004) Antimony(III) binding to humic substances: influence of pH and type of humic acid. Environ Sci Technol 38:4535–4541

Diao LP, Han RS, Pang L, Wang L (2010) Application of irregular soil geochemistry survey side of gully to prospect in the Puqing antimony–gold exploration area deposit, Guizhou, China. Geochim Cosmochim Acta 74:A230–A230

Ettler V, Mihaljevic M, Sebek O, Nechutný Z (2007) Antimony availability in highly polluted soils and sediments—a comparison of single extractions. Chemosphere 68:455–463

Filella M, Belzile N, Chen Y-W (2002a) Antimony in the environment: a review focused on natural waters: I. Occurrence. Earth-Sci Rev 57:125–176

Filella M, Belzile N, Chen Y-W (2002b) Antimony in the environment: a review focused on natural waters: II. Relevant solution chemistry. Earth-Sci Rev 59:265–285

Filella M, Belzile N, Lett M-C (2007) Antimony in the environment: a review focused on natural waters. III. Microbiota relevant interactions. Earth-Sci Rev 80:195–217

Hammel W, Debus R, Steubing L (2000) Mobility of antimony in soil and its availability to plants. Chemosphere 41:1791–1798

He M (2007) Distribution and phytoavailability of antimony at an antimony mining and smelting area, Hunan, China. Environ Geochem Health 29:209–219

He MC, Wan HY (2004) Distribution, speciation, toxicity and bioavailability of antimony in the environment. Prog Chem 16:131–135

He M, Wang X, Wu F, Fu Z (2012) Antimony pollution in China. Sci Total Environ 421–422:41–50

Ilgen AG, Trainor TP (2012) Sb(III) and Sb(V) sorption onto Al-rich phases: hydrous Al oxide and the clay minerals kaolinite KGa-1b and oxidized and reduced nontronite NAu-1. Environ Sci Technol 46:843–851

Jiang W, Zhang S, X-q S, Feng M, Zhu Y-G, McLaren RG (2005a) Sorption of arsenate on soils. Part 1: laboratory batch experiments using 16 Chinese soils with different physiochemical properties. Environ Pollut 138:278–284

Jiang W, Zhang SZ, Shan XQ, Feng MH, Zhu YG, McLaren RG (2005b) Sorption of arsenate on soils. Part 2: modeling the relationship between sorption capacity and soil physiochemical properties using 16 Chinese soils. Environ Pollut 138:285–289

Johnson CA, Moench H, Wersin P, Kugler P, Wenger C (2005) Solubility of antimony and other elements in samples taken from shooting ranges. J Environ Qual 34:248–254

Kang J, Hesterberg D, Osmond DL (2009) Soil organic matter effects on phosphorus sorption: a path analysis. Soil Sci Soc Am J 73:360–366

Krachler M, Emons H (2001) Speciation analysis of antimony by high-performance liquid chromatography inductively coupled plasma mass spectrometry using ultrasonic nebulization. Anal Chim Acta 429:125–133

Leuz A-K, Hug SJ, Wehrli B, Johnson CA (2006a) Iron-mediated oxidation of antimony(III) by oxygen and hydrogen peroxide compared to arsenic(III) oxidation. Environ Sci Technol 40:2565–2571

Leuz A-K, Mönch H, Johnson CA (2006b) Sorption of Sb(III) and Sb (V) to goethite: influence on Sb(III) oxidation and mobilization. Environ Sci Technol 40:7277–7282

Loeppert RH, Inskeep WP (1996) Iron. In: Sparks DL (ed) Methods of soil analysis, part 3. Chemical methods, SSSA Book Ser. No. 5. ASA, CSSA, SSSA, Madison, WI, pp 639–664

Luo X-S, Zhou D-M, Liu X-H, Wang Y-J (2006) Solid/solution partitioning and speciation of heavy metals in the contaminated agricultural soils around a copper mine in eastern Nanjing city, China. J Hazard Mater 131:19–27

Martínez-Lladó X, Valderrama C, Rovira M, Martí V, Giménez J, de Pablo J (2011) Sorption and mobility of Sb(V) in calcareous soils of Catalonia (NE Spain): batch and column experiments. Geoderma 160:468–476

Mehra OP, Jackson ML (1960) Iron oxide removal from soils and clays by a dithionite-citrate system buffered with sodium bicarbonate. In: Swineford A (ed) 7th National Conference on Clays and Clay Minerals. Adlard & Son Ltd, Washington, DC, pp 317–327

Mitsunobu S, Takahashi Y (2008) XAFS study on the behaviors of antimony and arsenic in soil-water system under various redox conditions. Geochim Cosmochim Acta 72:A638–A638

Mitsunobu S, Harada T, Hoshino K, Takahashi Y (2005) X-ray absorption study on the dominance of Sb(V) as secondary antimony species in soil. Chem Lett 34:1656–1657

Mitsunobu S, Takahashi Y, Terada Y, Sakata M (2010) Antimony(V) incorporation into synthetic ferrihydrite, goethite, and natural iron oxyhydroxides. Environ Sci Technol 44:3712–3718

Nakagawa T, Yuya M, Tachibana T, Takada Y, Nitani H, Emura S, Yamamoto TA (2005) XAFS study on site occupation of cobalt and iron in Z-type ferrite $Ba_3CO_2\text{-}xFe_{24}+xO_{41}$. J Magn Magn Mater 288:366–373

Nakamaru Y, Tagami K, Uchida S (2006) Antimony mobility in Japanese agricultural soils and the factors affecting antimony sorption behavior. Environ Pollut 141:321–326

Okkenhaug G, Zhu Y-G, Luo L, Lei M, Li X, Mulder J (2011) Distribution, speciation and availability of antimony (Sb) in soils and terrestrial plants from an active Sb mining area. Environ Pollut 159:2427–2434

Qi C, Liu G, Chou C-L, Zheng L (2008) Environmental geochemistry of antimony in Chinese coals. Sci Total Environ 389:225–234

Qi C, Wu F, Deng Q, Liu G, Mo C, Liu B, Zhu J (2011) Distribution and accumulation of antimony in plants in the super-large Sb deposit areas, China. Microchem J 97:44–51

Rakshit S, Sarkar D, Punamiya P, Datta R (2011) Antimony sorption at gibbsite–water interface. Chemosphere 84:480–483

Ruiz JM, Delgado A, Torrent J (1997) Iron-related phosphorus in overfertilized European soils. J Environ Qual 26:1548–1554

Shen DZ, Fan JX, Zhou WZ, Gao BY, Yue QY, Kang Q (2009) Sorption kinetics and isotherm of anionic dyes onto organo-bentonite from single and multisolute systems. J Hazard Mater 172:99–107

Smichowski P (2008) Antimony in the environment as a global pollutant: a review on analytical methodologies for its determination in atmospheric aerosols. Talanta 75:2–14

Sumner ME, Miller WP (1996) Cation exchange capacity, and exchange coefficients. In: Sparks DL (ed) Methods of soil analysis. Part 2: Chemical properties, 3rd edn. ASA, SSSA, CSSA, Madison, WI

Takaoka M, Fukutani S, Yamamoto T, Horiuchi M, Satta N, Takeda N, Oshita K, Yoneda M, Morisawa S, Tanaka T (2005) Determination of chemical form of antimony in contaminated soil around a smelter using X-ray absorption fine structure. Anal Sci 21:769–773

Tighe M, Ashley P, Lockwood P, Wilson S (2005a) Soil, water, and pasture enrichment of antimony and arsenic within a coastal floodplain system. Sci Total Environ 347:175–186

Tighe M, Lockwood P, Wilson S (2005b) Sorption of antimony(V) by floodplain soils, amorphous iron(III) hydroxide and humic acid. J Environ Monitor 7:1177–1185

Watkins R, Weiss D, Dubbin W, Peel K, Coles B, Arnold T (2006) Investigations into the kinetics and thermodynamics of Sb(III) sorption on goethite ([α]-FeOOH). J Colloid Interface Sci 303:639–646

Xi J-H, He M-C, Lin C-Y (2010) Adsorption of antimony(V) on kaolinite as a function of pH, ionic strength and humic acid. Environ Earth Sci 60:715–722